

**CHARACTERIZING SOLID STATE BATTERY DEGRADATION
USING OPTICAL MICROSCOPY AND OPERANDO X-RAY
TOMOGRAPHY**

Undergraduate Thesis
Presented to
The Academic Faculty

by

Dhruv Prakash

In Partial Fulfillment
of the Requirements for the
Undergraduate Research Option in
Materials Science and Engineering

Georgia Institute of Technology
May 2022


**CHARACTERIZING SOLID STATE BATTERY DEGRADATION
USING OPTICAL MICROSCOPY AND OPERANDO X-RAY
TOMOGRAPHY**

Approved by:

DocuSigned by:

E0A8A89F39BE4C8...

Dr. Matt McDowell, Advisor
School of Materials Science and Engineering
Georgia Institute of Technology

DocuSigned by:

69C860F784B442D...

Dr. Alena Alamgir
School of Materials Science and Engineering
Georgia Institute of Technology

DocuSigned by:

408CAE438468422...

Dr. Mary Lynn Realff
School of Materials Science and Engineering
Georgia Institute of Technology

Date Approved: 5/3/2022 | 10:51 AM EDT

Table of Contents

1. Introduction	1
2. Differences in Solid State Electrolytes	2
3. Degradation Mechanisms	3
1. Interfacial Resistance at the Anode	3
2. Short Circuiting Due to Dendritic Growth of Lithium	4
4. Experimental Methods	5
1. Optical Microscopy	5
2. X-Ray Tomography	8
5. Results and Discussion	10
1. Optical Microscopy	10
2. X-Ray Tomography	11
6. Conclusions	12
7. References	13

1. Introduction

With the need for renewable energy growing more prominent, it is necessary to develop safer and more energy dense batteries to store it. However, the energy density of current lithium-ion battery technology is nearing its physiochemical limit [1]. One proposed improvement is to replace the graphite anodes that are currently used with pure lithium metal. Because the energy stored in a battery is a function of how many ions the anode can hold, increasing the number of available lithium ions in the anode will allow the battery to hold more energy. Pure lithium anodes achieve just this by adding lithium atoms where there were previously graphene sheets, as illustrated by Figure 1. Furthermore, lithium movement throughout graphite is limited to a two-dimensional plane. In metallic lithium, however, lithium ions have access to a third direction for movements, resulting in less impedance to diffusion.

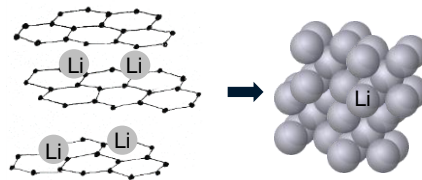


Figure 1: With graphite as an anode, lithium ions sit between graphene sheets (left). Instead, using pure lithium metal significantly increases the amount of lithium ions available to a battery.

While improving energy density, lithium metal anodes pose new problems for the battery. Given that pure lithium is very reactive, it can form electronically conductive dendrites that grow through the battery’s electrolyte and cause a short circuit [2]. Because the organic liquid electrolytes used in batteries are flammable, dendrite growth can be particularly dangerous. A safer alternative that has been proposed is the use of nonflammable, solid-state electrolytes (SSEs). However, following the mechanisms illustrated in Figure 2, SSEs may still react unfavorably with lithium. Void formation and, again, short circuiting dendrites lead to premature degradation of the solid-state battery (SSB).



Figure 2: On the left is a simple schematic of a cross-section of a solid-state battery (SSB). As illustrated on the right, charging and discharging the SSB can cause voids and dendrite growth at the interface between the lithium anode and the solid-state electrolyte (SSE).

There are a variety of solid materials that can conduct lithium ions, with many falling into the category of either sulfide or oxide ceramics. Sulfide electrolytes are characterized by the presence of sulfur atoms in the crystal lattice, whereas oxides contain oxygen. Functional electrolytes allow charged atoms to diffuse through them while still being electronically insulating. However, true electronic insulation is difficult to achieve, and the electronic conductivity that does exist is believed to be one cause of dendrite growth in SSBs [3]. Degradation mechanisms can generally differ from one SSE to the next depending on how the electrolyte thermodynamically reacts with lithium ions, but the most common degradation scenarios are outlined below. Understanding these mechanisms can help guide material selection for battery design for different applications. This, in turn, is an essential step in the efforts to prevent battery failure and bring SSBs to the market.

Because this degradation is a detriment to the battery's ability to store release charge, evidence of degradation can be found in its response to an electrical stimulus. However, to develop a more nuanced understanding of the mechanisms of degradation, it is helpful to look inside the battery and visualize the detrimental changes that take place. This study achieves this by using optical microscopy to document degradation across a two-dimensional cross-section of the battery. Three-dimensional scans were also taken with operando and ex-situ x-ray tomography, resulting in a more representative visual for the degradation mechanisms seen in electrical data. The solid electrolytes used in the studies was $\text{Li}_{10}\text{SnP}_2\text{S}_{12}$ (LSPS), a sulfide electrolyte with very high ionic conductivity similar to the superionic conductor $\text{Li}_{10}\text{GeP}_2\text{S}_{12}$ (LGPS) with the same crystal structure [4].

2. Differences in Solid State Electrolytes

Before discussing the degradation of SSBs in detail, it is important to note some of the differences seen in SSEs. The most obvious differences are those in ionic and electronic conductivity. The ionic conductivity tells us how well lithium ions flow through the solid electrolyte, and thus indicates the how easily a battery with that electrolyte charges and discharges. Furthermore, we want low electronic conductivities to prevent electronic current from bleeding through the battery.

Electronic conductivity also plays a role in battery degradation by reducing lithium ions into a neutral atom that will be stuck within the battery. In addition, different electrolytes undergo various electrochemical and thermodynamic reactions with lithium. These reactions result in an interphase that typically has worse ionic conductivity than the pure electrolyte. It is important to note that these reactions may be different under different electric potentials. Finally, there are also differences in shear strengths, and electrolyte particles with higher shear strengths are more mechanically stable. However, such electrolytes are also more brittle and can crack when too much mechanical stress is applied. Similarly, another factor that must be considered when placing electrolytes into battery systems is their macroscopic mechanical properties. Electrolytes are typically made as powders, and generally, oxide electrolyte particles are sintered into a single ceramic pellet. Such a pellet can shatter under stress. Sulfide electrolyte particles, on the other

hand, are often compressed into pellets without the addition of heat, and as a result, they are more compliant to stresses. Sulfides are not generally sintered because they must be contained in a controlled environment. They are unstable in air and produce toxic H_2S . Fortunately, they do not require sintering to display good ionic conductivity and are frequently implemented in batteries as just a green body [4, 5].

3. Degradation Mechanisms

Most degradation mechanisms seen in SSBs develop at the interface between pure lithium and SSE, and they result from both interfacial resistance and the growth of solid lithium dendrites that short circuit the battery. The two degradation mechanisms seem to be linked so it is important to understand the interplay between them. It must also be determined how variables set when cycling the SSB, namely current and time, affect this degradation.

1. Interfacial Resistance at the Anode

In an SSB, the anodic interface is the boundary where pure lithium metal from the anode meets the solid electrolyte. When the battery is being discharged, this interface is where lithium ions leave the anode and begin their journey towards the cathode. The ease with which this happens can be measured by the interfacial resistance. Some of the largest contributors to interfacial resistance, such as voids, cracks, and grain boundaries, cause a lack of interfacial contact where it is more difficult to transfer lithium to the SSE. These defects can show up when the battery is being manufactured if the electrolyte is not handled carefully or if its surface has not been polished. Hence, these issues can be attenuated by improving production parameters.

Other issues are more difficult to prevent. Because of lithium metal's reactivity, when lithium comes into contact with the electrolyte, a new phase is immediately formed [1]. This new interphase causes the electrolyte's volume to expand. This introduces a stress within the electrolyte at the interface, making it more susceptible to crack formation. This expanded interphase grows as the battery is cycled, so such cracks either become more likely to develop or are exacerbated [6]. This failure mechanism is typically seen in sintered oxide electrolytes like $Li_{1-x}Al_xGe_{2-x}(PO_4)_3$ (LAGP) and $Li_7La_3Zr_2O_{12}$ (LLZO) which are worse at elastically relieving stress like sulfide green bodies [6, 7].

Furthermore, interfacial contact between electrolyte and lithium can also decrease because of the formation of voids. This is a degradation mechanism seen in both sulfide and oxide electrolytes. Voids form when lithium is stripped from the anodic interface while the battery is being discharged. If the volumes where lithium was taken from are not replaced by other lithium atoms, or SSE particles in the case of sulfides, these voids can become permanent and interfacial contact is decreased [8]. A popular solution to preventing the formation of voids is to compress the battery while it is cycled. This added stack pressure helps quench voids by making it easier for other lithium atoms, or sulfide SSE particles, to take the stripped lithium's place [5, 9]. Stack pressure has also been shown to improve general interfacial contact that results from cracks or surface roughness [8].

Both crack and void formation also seem to be dependent on the current density at which the battery is cycled. Interphase growth has been shown to be significantly less uniform at higher current densities ($>0.5 \text{ mA/cm}^2$) leading to a non-uniform distribution of stresses across the SSE. This makes cracks more likely to develop and propagate and causes the battery to fail more quickly [10]. A similar phenomenon dictates the relationship between current density and void formation. When discharging at higher current densities, more lithium is stripped at the interface, and the rapid formation of the resulting voids cannot be as easily counteracted by increasing stack pressure [5, 9]. Crack and void formation becomes worse over many cycles even if the current pushed through the SSB does not change. This is because, as cracks and voids form, there is a decrease in the areas at the interface where there is contact enough to allow lithium to be plated and stripped. Because the current does not change, less interfacial contact means higher current densities where there is contact, and this increase in current density results in the formation of more voids and more crack inducing interphase [9].

2. Short Circuiting Due to Dendritic Growth of Lithium

When charging an SSB, lithium ions return from the cathode to the anodic interface where they recombine with electrons and are plated as lithium metal. However, if contact between the anode and SSE is not uniform, lithium is not plated equally across the interface. The regions where there is good contact see a higher electric field density. This forces a lot of lithium to be deposited in those areas, resulting in a root-like morphology of lithium metal throughout the SSE known as dendrites. Whenever the battery is charged, there is preferential lithium deposition at the tips of the dendrite, where there is a higher electric field flux ^[5]. Eventually, these lithium metal dendrites grow long enough to reach the cathode. Because lithium metal is electronically conductive, this causes the battery to short circuit. Dendrites have been shown to grow from points at the anodic interface where contact is good and the electric field is denser. Thus, for dendrites to occur, interfacial resistance is typically a prerequisite [11].

Just like interfacial resistance, dendrite growth seems closely correlated with current density [3, 12]. At high current densities, ion movement is more inhibited by kinetic barriers, and plating on existing dendrites is the path of least resistance [3, 12]. Furthermore, dendrite growth is often seen around the borders of SSE grains, so it seems that the path of least resistance typically follows grain boundaries. However, Porz et al. were able to show that dendrites will grow even when the SSE is monocrystalline and no grain boundaries exist. Although the critical current density at which dendrites began to form was higher in the single crystal SSE, it remained under the target current densities of $>1 \text{ mA/cm}^2$ required for SSBs to be commercially viable [12]. To further complicate matters, Han et al. were able to use neutron depth profiling to confirm that dendrites can grow from nucleation sites within the bulk of the SSE as well. Because, for lithium to be deposited onto a dendrite, electrons must be present, this discovery indicates that above certain current densities, some free electrons flow through the SSE [3]. Thus, when selecting an SSE, electronic conductivity must be considered.

4. Experimental Methods

To analyze the reaction between the SSE and solid lithium under electrochemical conditions, we used symmetric cells using only these two materials. As opposed to full cells that contain an anode and a cathode separated by an electrolyte, symmetric cells have the same electrode on both sides, allowing us to look exclusively at the reaction between the lithium and the electrolyte. For our experiments, we used the sulfide electrolyte $\text{Li}_{10}\text{SnP}_2\text{S}_{12}$ (LSPS) which has the same crystal structure as the superionic conductor $\text{Li}_{10}\text{GeP}_2\text{S}_{12}$ (LGPS) but is cheaper to produce.

Traditionally, symmetric cells are built based on the geometry shown in Figure 4. Because the reaction between the electrolyte and lithium occurs where the two meet, we need to look inside the cell to examine the cell's degradation. One way to achieve this is to use x-ray tomography to create a three-dimensional scan of the cell at different stages as lithium is moved through the LSPS. This is the technique Tippens et al. used with the oxide LAGP [6]. However, to use tomography to view the reaction while measuring electrochemistry is very time consuming. Tomography scans can take multiple hours, and because they require the sample to rotate, electrochemical test needs to be paused whenever a scan is taken.

Optical microscopy, a more time efficient characterization technique could be used in tandem with x-ray tomography for initial characterizations of degradation phenomena. Operando optical microscopy allows us to take two dimensional pictures of the cell at certain intervals of time and does not require us to pause the electrochemistry. A significant hurdle accompanying this method is that it only provides information about a surface, and the reaction in a symmetrical cell occurs throughout a volume that is inaccessible to visible light. While a 2D image does not give us as much information as a 3D scan, it is easier to analyze changes that occur over time. For this reason, an experiment using optical microscopy was developed to be used as a more accessible characterization method that was later supplemented by more precise x-ray tomography data.

1. Optical Microscopy

We developed a novel symmetric cell geometry that allows us to use optical microscopy to view the growth of interphase in real time. In this new design, shown in Figure 3, we place both

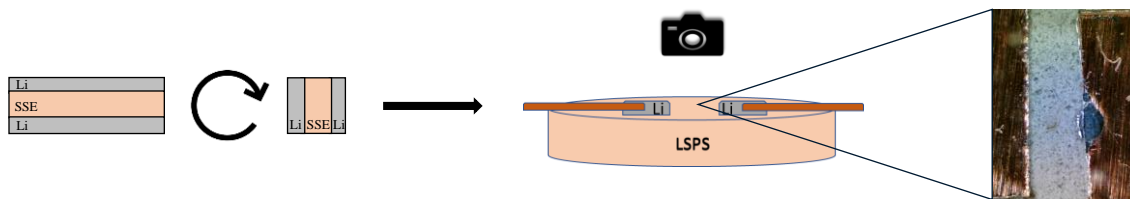


Figure 3 The novel optical microscopy cell (right) resembles the traditional symmetric cell (left) rotated upon its side.

lithium current collectors on the same side of the LSPS pellet, separating them by three millimeters. By doing this, we hope to replicate the same degradation mechanism witnessed in traditional symmetric cells.

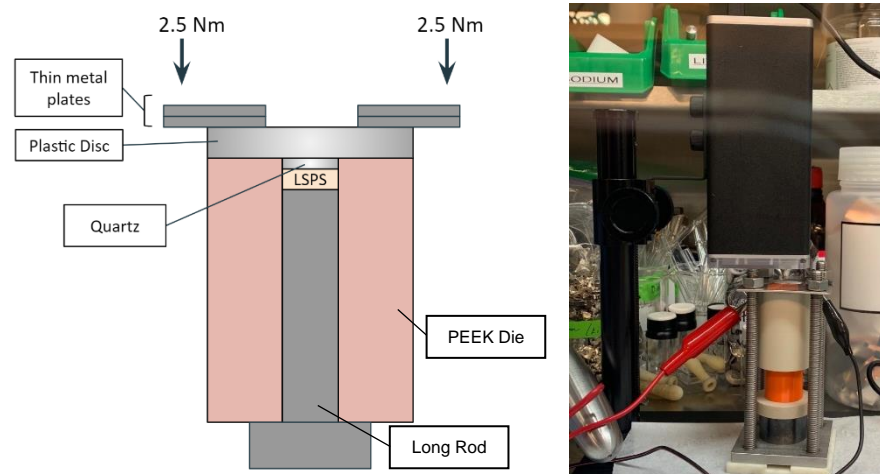


Figure 4: Illustration of optical microscopy cell (left). Picture of an optical microscopy cell during testing (right).

The cell is completely built and tested inside a glovebox. First the LSPS pellet is pressed inside a cylindrical PEEK die with an internal diameter of 1 cm. To press the LSPS, a short steel rod is taped to one side of the die such that its surface is level with the opening in the die. After massing out 90 milligrams of LSPS powder, the electrolyte was carefully poured into the die from the opening on the other side. The short rod should prevent any powder from falling out. At this point, it is important to ensure that the LSPS is uniformly distributed on the rod to keep the pellet from breaking when it is pressed. A longer steel rod is then slowly inserted into the die from the same side LSPS was just poured in. The powder is now trapped in between the steel rods and the walls of the die. The die, along with the rods, is then pressurized using a single axis hydraulic press to a pressure of 8 MPa. The short rod is removed. The surface of the pellet should be nearly level with the opening of the die, and no visible cracks or imperfections should be visible.

To prepare the electrodes, a 3 cm square of copper foil is brought into the glove box, and a strip of electrical tape is placed along the middle of the foil. When these electrodes are placed on the LSPS pellet, all the current should only be transferred through the lithium. The tape prevents the copper foil from contacting the LSPS pellet and depositing electrons. A square centimeter of lithium is then cleaned by scraping it with a Teflon block. The lithium is then spread on the same side as the tape. Only a 1 cm wide strip is covered with lithium, and the remaining copper foil is left clean. The lithium should only be 0.25 to 0.5 millimeters thick. Multiple electrodes can now be cut from this copper sheet. Each electrode should be 3 mm wide and have a 2 mm by 3 mm rectangle of lithium.

Two electrodes are then placed on the side of the LSPS pellet where the short rod was previously. The long rod should remain in the die because it is needed to pressurize the electrodes on the pellet later. The lithium should be completely on top of the electrolyte, and a 3 mm gap is left between the two electrodes. The copper “tail” of each electrode should fall over the sides of the die. A 0.7 cm square of quartz glass is then carefully placed on both electrodes ensuring that the electrodes maintain contact with the electrolyte. A plastic circle with a 2 cm diameter is then placed top of the glass.

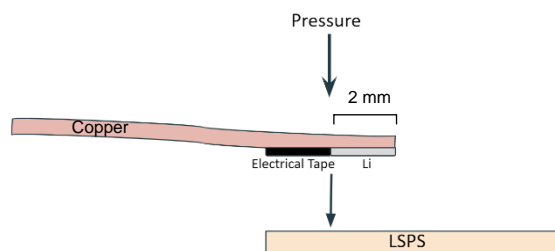


Figure 5: Placement of one electrode onto LSPS pellet.

The setup is pressurized between two square steel plates. Each plate has a hole in each corner through which four bolts are passed through. These bolts run through the bottom plate, around the PEEK die, and then through the top plate. The top plate is thinner than the bottom plate and has a 1.5 cm diameter hole at its center. This central hole is lined up over the plastic circle so that through this hole the two electrodes and the LSPS pellet are visible. The edge of the plastic circle should be completely under the metal plate to ensure uniform pressure is applied to the electrodes and electrolyte. Figure 4 depicts what the final setup should look like. Nuts are screwed on the bolts above the top plate. These nuts are carefully tightened to a torque of 2.5 newton-meters, with higher torque corresponding to more pressure. If pressure is ever nonuniformly applied by the four nuts, the quartz may shatter.

The copper “tails” of each electrode should still be intact and connected to the lithium ends. These are connected to a Biologic potentiostat to run the electrochemical test. The potentiostat is set to control the current and read the electric potential difference between each electrode. A voltage limit of 4V and -4V is set to prevent reactions that happen at potentials that a battery would not typically reach. Thus, whenever the potential reaches either 4V or -4V, we program the current to change direction.

As the electrochemistry is being run, an optical microscope takes pictures of the region between the electrodes. The microscope was kept inside the glovebox and was set to take a picture every 4 seconds. These pictures were then converted into a time-lapse using ImageJ.

However, it soon became clear that a major challenge associated with this technique was applying enough pressure to the electrodes. The overpotential, or the difference in the theoretical and experimental electric potential once a current is applied to the cell, is widely used as an indicator of how well a cell will cycle. The theoretical potential for symmetric cells initially is zero because there should not be any potential difference between the lithium electrodes—they are the same material. The overpotential of traditional symmetric cells is very low at nearly 0.25 V. Unfortunately, we saw that the initial electric potential was consistently high, between 0.5 and 1.5 V. We noticed that as more pressure was added to the cell, the overpotential decreased.

After 3 newton meters of torque, we could no longer add more pressure to the cell because the quartz glass would shatter, rendering the cell useless. To prevent this from happening, we tried to replace the glass with plastic circles cut from a petri dish. This did not significantly improve the overpotential, and the image quality decreased. We also attempted to fix this by replacing the top metal plate with a thicker fiber glass plate. Because this top metal plate began to bend at higher pressures, we believed that this bending applied uneven pressure to the quartz, causing it to shatter. We hoped a solid fiber glass piece would prevent this, but the fiber glass also began to bend. Overpotential did not decrease either.

2. X-Ray Tomography

To provide a complete story of how sulfide batteries degrade, optical microscopy needs to be accompanied by x-ray tomography. Additionally, x-ray tomography should be used to analyze full cell degradation to identify how degradation may differ in the presence of a cathode. X-Ray tomography experiments were of symmetric cells with the solid electrolyte LSPS.

An illustration of the cell casing used is shown in Figure 6. This cell casing was designed such that the cell was only 2 mm in diameter, allowing the whole cell to be imaged by the narrow x-ray beam. Furthermore, the casing allowed us to seal the air-sensitive cell when it was pressurized, preventing the cell's degradation when being imaged in ambient air.

The cells were made by first pouring 7 mg of LSPS into the casing and forming it into a pellet by applying a pressure of 225 MPa. The resulting green body was roughly 1 mm thick and 2mm in diameter. To completely cover each surface of the pellet, 2 mm diameter lithium foil circles were punched out and attached to steel rods that were inserted into the casing. These rods were then pushed together by screws that were tightened to 0.25 Nm. This corresponds to about 10 MPa or pressure on the newly formed symmetric. To prevent the rotating screws from rotating the steel rods and thus applying a torque onto the cell, graphite foil was added as a lubricant between the screws and the steel rods. This assembly was done in an argon environment inside a glove box.

Monochromatic x-ray imaging was conducted at Argonne National Lab's Advanced Photon Source (APS). The x-rays had an energy of 28 keV.

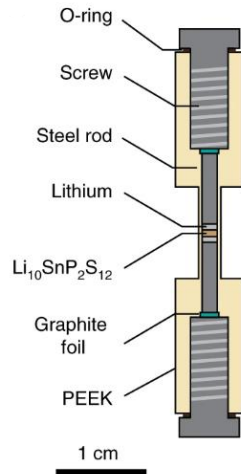


Figure 6: X-Ray tomography cell cross-section. Taken from Lewis et al. [9].

During imaging, the symmetric cell was cycled using a Bio-Logic SP-150 potentiostat. While current densities were between 1 mA cm^{-2} and 4 mA cm^{-2} for each scan, about 4 mAh cm^{-2} of lithium was plated during each half cycle.

5. Results and Discussion

1. Optical Microscopy

Based on the electrochemical data and the images collected, the novel cell geometry of the optical microscopy cell shows promise as a new way of analyzing the degradation mechanism of symmetric cells. However, the difficulties of this method, as noted in the methods sections, limited a conclusive optical microscopy study.

Figure 7 shows a successful imaging experiment. This image allows us to compare the region between electrodes before a cell was cycled and after. The growth of darker colored regions indicates that an interphase has grown between the lithium and the solid electrolyte. The dark black streaks, circled in red in the figure, show that dendrites developed overtime. This provides evidence that short circuiting due to dendritic lithium metal growth through the solid-state electrolyte leads to battery failure. The figure also shows the non-uniform interface between lithium metal and the electrolyte. Certain areas under the copper had more lithium which, when pressed onto the pellet, caused the lithium to spread out. As a result, pressure and interfacial contact is not uniform across the cell. Furthermore, the distance between the two electrodes seems to vary along the length of the imaged window. Because of these issues, as well as the high overpotentials, this optical microscopy method did not seem to provide a thorough characterization of degradation.

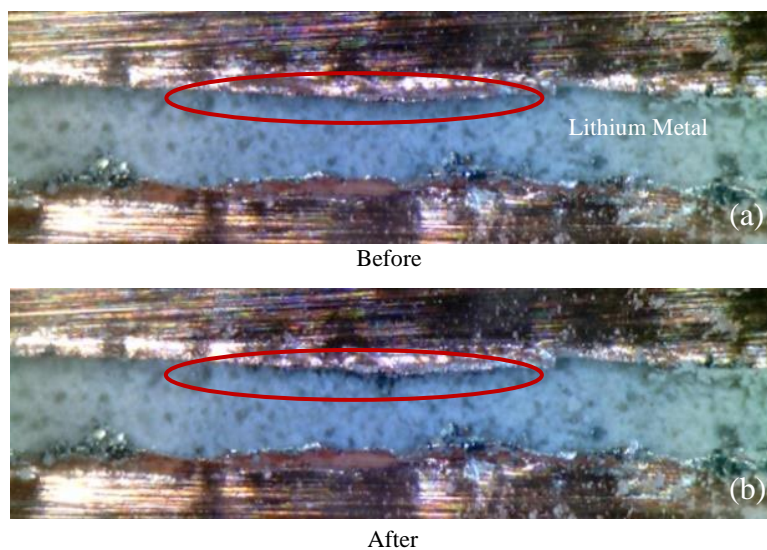


Figure 7: (a) Before and (b) after images of the electrolyte show interphase growth in the area marked by the red ellipse. The lithium electrodes are compressed under the copper leads at the top and bottom of each picture. The dark black regions are the dendritic growth of lithium through the electrolyte.

2. X-Ray Tomography

The symmetric cells run for the tomography scans better elucidated these degradation mechanisms associated with LSPS. As shown in Figure 9, when cycled at a constant current density of 1 mA/cm^2 , the potential across the electrolyte aggressively diverged from the ideal symmetric cell potential of 0 V. This occurred during the second lithiation when the current was reversed, and it indicates that the impedance to Li^+ diffusion grew with time.

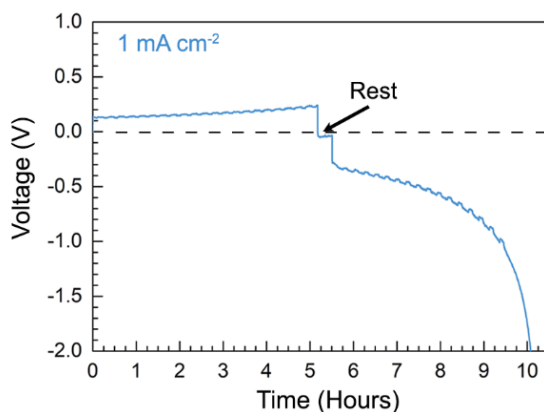


Figure 8: Cycled at 1 mA/cm^2 , this cell failed in its second lithiation due to a large impedance. Taken from Lewis et al. [9].

This increase in impedance was explained by the x-ray images generated of the interphase of this cell shown in Figure 10. Before it was cycled, an interphase between lithium metal and LSPS can already be seen. The galvanostatic cycling at 1 mA/cm^2 seems to have led to interphase growth and to contact loss. The interface in this figure was the one initially delithiated, so these images and data show that delithiation can remove contact between the lithium anode and LSPS. The loss of contact is a kinetic barrier to the diffusion of lithium to the other electrode, and in turn, the battery can no longer be cycled reliably.

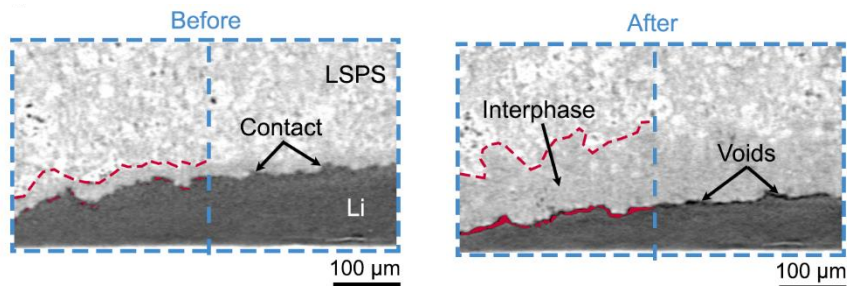


Figure 9: X-Ray images of cell before and after being cycled at 1 mA/cm^2 . This corresponds to the data shown in Figure 9. Note the growth of interphase and contact loss. Taken from Lewis et al. [9].

6. Conclusions

These experiments have highlighted two degradation mechanisms associated with solid state batteries made with the electrolyte LSPS and a lithium metal anode. Optical microscopy experiments provided evidence of the growth of interphase and dendrites. X-Ray tomography provided further electrochemical and visual evidence, showing interfacial contact between anode and electrolyte can be lost during delithiation. Both the discussed degradation mechanisms seem to result from non-uniform current flow across the cross section of the battery. When the SSB is being discharged, such current can contribute to void formation because current concentrations remove lithium from the interface faster than it can be replaced by diffusion from underneath. As a result, non-uniformities are exacerbated as nonuniform interfacial contact leads to phenomena that continue to reduce contact. During charging, on the other hand, short circuiting dendrites are formed at points where there is better contact, and thus, a higher current density. These degradation mechanisms both correspond to the anodic lithium metal-LSPS interface and seem to be worsened at higher overall current densities.

In addition to current density, the capacity, or amount of charge, transferred between electrodes during each cycle is an important variable in relation to dendrite formation not considered in this work. Following the tomography data discussed in this thesis, Lewis et al. were able to deconvolute the relationship between current density, capacity, and dendrite formation. It was determined that dendrite formation enough to initiate short circuiting in the SSB begins near a threshold capacity for each cycle, and the threshold capacity varies with the current density used [13]. Because of the phenomena discussed in this work, current density increases as SSBs are cycled, and as a result, the threshold capacity for each cycle must fall over the course of the battery's life. As further work is done to better understand the emergence of current limiting defects, we must try to look at it through the lens of capacity as well.

7. References

- [1] J. Janek and W. G. Zeier, "A solid future for battery development," (in English), *Nat Energy*, vol. 1, Sep 8 2016, doi: Artn 16141
10.1038/Nenergy.2016.141.
- [2] K. N. Wood *et al.*, "Dendrites and Pits: Untangling the Complex Behavior of Lithium Metal Anodes through Operando Video Microscopy," (in English), *Acs Central Sci*, vol. 2, no. 11, pp. 790-801, Nov 23 2016, doi: 10.1021/acscentsci.6b00260.
- [3] F. D. Han *et al.*, "High electronic conductivity as the origin of lithium dendrite formation within solid electrolytes," (in English), *Nat Energy*, vol. 4, no. 3, pp. 187-196, Mar 2019, doi: 10.1038/s41560-018-0312-z.
- [4] N. Kamaya *et al.*, "A lithium superionic conductor," (in English), *Nature Materials*, vol. 10, no. 9, pp. 682-686, Sep 2011, doi: 10.1038/Nmat3066.
- [5] C. Hänsel and D. Kundu, "The Stack Pressure Dilemma in Sulfide Electrolyte Based Li Metal Solid-State Batteries: A Case Study with Li6PS5Cl Solid Electrolyte," *Advanced Materials Interfaces*, <https://doi.org/10.1002/admi.202100206> vol. n/a, no. n/a, p. 2100206, 2021/04/01 2021, doi: <https://doi.org/10.1002/admi.202100206>.
- [6] J. Tippens *et al.*, "Visualizing Chemomechanical Degradation of a Solid-State Battery Electrolyte," (in English), *Acs Energy Lett*, vol. 4, no. 6, pp. 1475-1483, Jun 2019, doi: 10.1021/acseenergylett.9b00816.
- [7] S. Y. Han *et al.*, "Porous Metals from Chemical Dealloying for Solid-State Battery Anodes," (in English), *Chem Mater*, vol. 32, no. 6, pp. 2461-2469, Mar 24 2020, doi: 10.1021/acs.chemmater.9b04992.
- [8] M. J. Wang, R. Choudhury, and J. Sakamoto, "Characterizing the Li-Solid-Electrolyte Interface Dynamics as a Function of Stack Pressure and Current Density," (in English), *Joule*, vol. 3, no. 9, pp. 2165-2178, Sep 18 2019, doi: 10.1016/j.joule.2019.06.017.
- [9] J. A. Lewis *et al.*, "Linking void and interphase evolution to electrochemistry in solid-state batteries using operando X-ray tomography," *Nature Materials*, 2021/01/28 2021, doi: 10.1038/s41563-020-00903-2.
- [10] J. A. Lewis *et al.*, "Interphase Morphology between a Solid-State Electrolyte and Lithium Controls Cell Failure," (in English), *Acs Energy Lett*, vol. 4, no. 2, pp. 591-599, Feb 2019, doi: 10.1021/acseenergylett.9b00093.
- [11] J. A. Lewis, J. Tippens, F. J. Q. Cortes, and M. T. McDowell, "Chemo-Mechanical Challenges in Solid-State Batteries," (in English), *Trends Chem*, vol. 1, no. 9, pp. 845-857, Dec 2019, doi: 10.1016/j.trechm.2019.06.013.
- [12] A. Sharafi, C. G. Haslam, R. D. Kerns, J. Wolfenstine, and J. Sakamoto, "Controlling and correlating the effect of grain size with the mechanical and electrochemical properties of Li7La3Zr2O12 solid-state electrolyte," (in English), *J Mater Chem A*, vol. 5, no. 40, pp. 21491-21504, Oct 28 2017, doi: 10.1039/c7ta06790a.
- [13] J. A. Lewis *et al.*, "Role of Areal Capacity in Determining Short Circuiting of Sulfide-Based Solid-State Batteries," *ACS Applied Materials & Interfaces*, vol. 14, no. 3, pp. 4051-4060, 2022/01/26 2022, doi: 10.1021/acsami.1c20139.